NATIONAL TRANSPORTATION SAFETY BOARD

Washington, D.C.

Aircraft Performance
Group Chairman's Aircraft Performance Study
American Airlines flight 903
Dated June 30, 1998

(39 Pages)

1

NATIONAL TRANSPORTATION SAFETY BOARD

Office of Research and Engineering
Washington, D.C. 20594

June 30, 1998

Aircraft Performance

Group Chairman's Aircraft Performance Study

by John O'Callaghan

ACCIDENT

Location: West Palm Beach, Florida

Date: May 12, 1997

Time: 1929 Universal Coordinated Time (UTC)
                 1529 Eastern Daylight Time (EDT)

Flight: American Airlines Flight 903

Aircraft: Airbus A300B4-605R, Registration #N90070

NTSB#:   **DCA97MA049**

TABLE OF CONTENTS

④

NATIONAL TRANSPORTATION SAFETY BOARD

Office of Research and Engineering
Washington, D.C. 20594

June 30, 1998

Aircraft Performance

Group Chairman's Aircraft Performance Study
by John O'Callaghan

A. ACCIDENT

Location:	West Palm Beach, Florida
Date:	May 12, 1997
Time:	1929 Universal Coordinated Time (UTC)
	1529 Eastern Daylight Time (EDT)
Flight:	American Airlines Flight 903
Aircraft:	Airbus A300B4-605R, Registration #N90070
NTSB#:	DCA97MA049

B. GROUP

Chairman: John O'Callaghan
              National Transportation Safety Board
              Washington, D.C.

Member: Dominique Buisson
              Airbus Industrie
              Blagnac, France

Member: John DeWald
              American Airlines
              DFW Airport, Texas

Member: Franck Giraud
              Bureau Enquetes-Accidents
              Le Bourget, France

Member: Don Pitts
              Allied Pilots Association
              Tulsa, Oklahoma

Member: Guy Thiel
              Federal Aviation Administration
              Lakewood, California

C.   SUMMARY

History of Flight

On May 12, 1997, at 1929 UTC, American Airlines Flight 903, an Airbus A300B4-605R (registration N90070), experienced an in flight upset about 10 miles North of HEATT intersection near West Palm Beach, Florida. One passenger sustained serious injuries and the airplane received minor damage. The crew declared an emergency and landed at Miami International Airport without further incident. The flight originated from Logan International Airport in Boston, Massachusetts, about 2 hours and 16 minutes before the upset.

Role of the Aircraft Performance Group in the Accident Investigation

The Aircraft Performance Group for this accident was formed during an organizational meeting held at NTSB headquarters in Washington, D.C. on June 26, 1997.

The purpose of the Aircraft Performance Group (ACPG) is to determine and analyze the motion of the aircraft and its response to control inputs. In particular, the ACPG attempts to define the aircraft position and attitude throughout the flight, determine its flight path with respect to the air and the ground, and compare these motions with the known or expected aircraft performance and handling qualities. The data the ACPG uses to obtain this information includes but is not limited to the following:

- Approach and airport surveillance (ASR) radar data.
- Digital Flight Data Recorder (DFDR) data.
- Cockpit Voice Recorder (CVR) information.
- Meteorological information.
- Known or predicted aircraft dynamic characteristics as determined from wind tunnel tests, flight tests, and analysis.
- Evaluations of predicted aircraft performance via simulation.

This aircraft performance study describes the results of using the information sources listed above in defining, as far as possible, the motion of AA903, and of reconciling that motion with the established flight characteristics of the A300.

Areas of Study and Findings

The motion of the accident aircraft is almost completely defined by the data recorded on the DFDR. The main objective of this Study is to determine if that motion represents the normal, expected behavior of the aircraft, and if not, why not. An essential tool in this task is the engineering simulator, which represents the manufacturer's best knowledge of the aircraft behavior.

Much of the analysis in this Study is devoted to an attempt to understand and resolve the differences between the aircraft roll behavior just prior to the upset as recorded by the DFDR, and the expected roll behavior of the A300 as predicted by the engineering flight simulator. As part of this effort, the effect of an "atmospheric disturbance" on the aircraft dynamics is discussed, and the role of such a disturbance in the upset scenario is evaluated. The limits of simulator model and DFDR data accuracies are also considered.

This Study also discusses the effects of various upset recovery techniques on the magnitude and character of the aircraft motions immediately after the first upset event.

The ACPG was unable to resolve conclusively the differences between the roll behavior of the aircraft recorded by the DFDR, and the behavior predicted by the simulator. The group found that according to wind tunnel and flight tests performed by Airbus Industrie during the development of the A300, the simulator should represent the aircraft adequately at angles of attack (α) below 9°. The Group also found that an external rolling moment not present in the aerodynamic models of the A300 is required for the simulation to match approximately the rolling motion recorded by the DFDR, even at $\alpha < 9°$. However, an analysis of the DFDR information shows little evidence of an atmospheric disturbance in α, speed, or load factor data.

There is insufficient information available to evaluate other possible sources of an external rolling moment, such as asymmetrical wing contamination due to icing. For these reasons, it cannot be determined whether or not the disagreement between the simulator and DFDR is due to limitations in the simulator model of the aircraft at high α, an encounter with an atmospheric disturbance, a combination of these effects, or some other cause. Nonetheless, by treating the unexpected roll behavior of the aircraft just prior to the main upset as a bank angle disturbance (by whatever cause), and by evaluating the effect of that disturbance on the mechanics of the upset, the behavior of the aircraft throughout the upset sequence can be understood well.

From this macroscopic point of view, then, the upset sequence can be described as a slow deceleration after leveling off from a descent, followed by a continued deceleration in a turn and a subsequent asymmetrical stall of both wings, followed by a recovery involving secondary stalls and large amplitude oscillations in lateral, longitudinal, and directional controls and attitudes. The final recovery of airspeed and angle of attack is achieved through the longitudinal acceleration provided by thrust and the nose down pitch attitude resulting from the series of stalls. The effect of the bank angle disturbance just prior to the first stall was to accelerate the rate of increase of angle of attack and hasten the stall by increasing the bank angle and creating a greater demand for lift in order to maintain altitude.

In order to evaluate the effect of the bank angle disturbance at a higher airspeed, it was assumed that the disturbance was caused by an atmospheric perturbation that caused an asymmetrical lift distribution over the wings. A perturbation that produced the required rolling moments was then modeled and tested in an Airbus engineering simulator. The group found that at the recommended operating speed of 210 KIAS, an encounter with the perturbation resulted in a bank angle disturbance but that there was sufficient α margin to stall that the event was controlled easily by the autopilot.

The effect of stall recovery techniques on the motion of the aircraft during the upset was evaluated in the simulator by encountering the perturbation while duplicating the accident conditions. The Group determined that recovering from the stall by first lowering the nose and reducing the angle of attack will improve the effectiveness of the lateral controls and enable the wings to be leveled without using the rudder, or by using the rudder only to coordinate the maneuver. The Group also found that large rudder deflections at high α produce very large lateral accelerations and roll rates while inducing even higher angles of attack and delaying the stall recovery.

D.   DETAILS OF THE INVESTIGATION

I. Introduction

As mentioned above, the purpose of the ACPG is to define the motion of the aircraft, compare that motion with theoretical predictions based on knowledge of the aircraft design and performance characteristics, and to resolve any differences between the two. The approximate actual motion of the aircraft is recorded in the DFDR data. The "theoretical predictions" of aircraft motion are provided by the engineering simulator, which uses mathematical models of the Earth and the aircraft to calculate forces and moments and solve the equations of motion to determine the aircraft position and attitude as a function of time.

Simulator predictions of the motion of AAL903 agree well with the data recorded by the DFDR until shortly before the first nose-down pitching motion of the upset. At this point, the simulator predicts the aircraft should have arrested a roll to the right and started to roll left back to wings level, while the DFDR data shows the aircraft continued to roll to the right until stopped by a large left rudder deflection just prior to the first nose-down pitching motion of the upset.

The first nose-down pitching motion of the upset occurs at a time where the angle of attack exceeds the angle of attack for maximum lift, and by definition the aircraft is stalled. During the subsequent recovery from the stall, the rapid, large oscillations in the attitude of the aircraft and the high angles of attack and sideslip make comparisons of the recorded motion with simulator predictions of the motion difficult, both because of limitations in the mathematical modeling of the simulator, and because of difficulties with the accuracy of the DFDR data under such dynamic conditions.

The upset event can therefore be divided and analyzed in two parts, corresponding to the times before and after the first exceedance of the stall angle of attack (the first stall). The DFDR recorded motion before the first stall is smooth and corresponds to a flight regime where the simulator models should be valid, and so the simulator can be used to analyze this part of the aircraft motion. The very dynamic motion after the first stall can not be analyzed quantitatively with the simulator, and so must be examined from a more qualitative point of view. The disagreement between the DFDR and the simulator occurs very near the border between these two parts of the upset, shortly before the first stall.

Organization of this Performance Study

The remainder of this Study will present the DFDR and radar data for this accident, show the simulator predictions of the aircraft motion prior to the first stall, explore possible explanations of differences between the simulator and the DFDR results, evaluate the effect of the roll disturbance on the mechanism of the first stall, and discuss qualitatively the character of the aircraft motion after the first stall and the effects of recovery techniques on that motion.

Section D-II presents various parameters recorded by the DFDR and contains a chronology of the upset event condensed from the chronology given in the Flight Data Recorder Group Chairman's Factual Report. The radar data for the flight is also presented and compared with position information recorded by the DFDR.

Section D-III describes the simulator matches of the event performed by Airbus Industrie for the portion of the event prior to the first stall. The disagreement with the DFDR roll angle just prior to the stall is shown, as is the ability of an external rolling moment and moderate wind shear to resolve the disagreement.

Section D-IV contains a qualitative discussion of the motion of the aircraft between the first stall and the final recovery to level flight, and the consistency of that motion with expected aircraft behavior in that flight regime.

Section D-V explores possible explanations for the difference in roll behavior between the simulator and DFDR, including limitations in simulator fidelity and an encounter with an atmospheric disturbance. The consistency of the simulator with wind tunnel and flight tests is discussed, as is the consistency of an atmospheric disturbance with other DFDR parameters, the history of the accident flight, and the experience of other flights in the area.

Section D-VI discusses the role of the bank angle upset, identified by the disagreement between the DFDR and the simulator, in the mechanism of the first stall. The effect of encountering the bank angle upset at a higher airspeed is also discussed.

Finally, Section D-VII discusses the effect of stall recovery technique on the motions of the aircraft after the first stall. The ACPG's simulator work in this area is also presented.

Much of the data presented in Section E is based on, or derived, from parameters recorded on the DFDR, while not being recorded directly by the DFDR. Detailed derivations of the equations used to calculate this data are presented in the Appendix.

II. Data Description and Presentation

Cockpit Voice Recorder Data

Because the upset event occurred more than half an hour before the aircraft landed at Miami, the cockpit voice recorder information for the upset portion of the flight was overwritten. Thus the CVR provided no useful information regarding aircraft performance during the upset.

Radar Data

American Flight 903 was tracked by the Miami Air Route Traffic Control Center (ARTCC) radar system. The radar antennas of the system rotate once every 12 seconds, resulting in a return signal from the aircraft at the same rate. Altitude information is received from the aircraft's transponder, which encodes altitude based on atmospheric pressure measured by the aircraft pitot-static system. Since the radar and DFDR receive their altitude information from the same raw data source, the altitude recorded by the two devices should agree well and can be used to synchronize the radar and DFDR information in time.

Figures 1a and 1b present a comparison of the position of the aircraft as measured by the ARTCC radar with the position recorded by the aircraft DFDR. The position is presented as nautical miles (NM) North and East of HEATT intersection, located at 26° 29' 27.5" North Latitude, 79° 56' 46.3" West Longitude (about 14 NM Southeast of Palm Beach International Airport). Figure 1a shows that the radar data agrees with the DFDR data to within about 0.5 NM.

As expected, the altitude data recorded by the radar and the DFDR agree very well. The transponder rounds the altitude to the nearest 100 ft., and so the radar altitude information has an uncertainty of ±50 ft. Figure 1a shows that for about a minute and a half after the upset (corresponding to the altitude deviation between Elapsed Time (ET) = 60 s. and ET = 150 s.), the radar did not receive transponder altitude information.

The radar and DFDR altitude traces have been used to correlate the times of the DFDR and radar sites. Both DFDR and Miami ATC time have been converted to an Elapsed Time reference for convenience. The relationship between DFDR time, Miami ATC (radar) time, and Elapsed Time is as follows:

Elapsed Time	=	DFDR Time	=	MIA ATC Time
0.0 s.		3220.0 s.		19:28:20 UTC

Figure 1b shows a three-dimensional view of the radar and DFDR position data. The projections of the 3D curves and points onto the East-North and East-Altitude planes are also shown.

Digital Flight Data Recorder (DFDR) Data

The A300 involved in this accident was equipped with a modern DFDR that recorded about 200 parameters, which define the motion of the aircraft almost completely. A description of the DFDR and the recorder readout process can be found in the Flight Data Recorder Group Chairman's Factual Report. The DFDR readout provides tabulated and plotted values of the recorded flight parameters versus time. Tables of all the recorded parameters for the upset event, and plots of most of them, are included in the FDR Factual Report. The plots of the data in the FDR Factual Report are reproduced here as Figures 2a-2f for easy reference.

Because much of this Performance Study will focus on the 55 seconds of the flight prior to and including the first stall, detailed plots of the DFDR parameters most relevant to aircraft performance during this time are plotted in Figures 3a - 3f. Also plotted in these Figures are parameters not recorded directly by the DFDR, but calculated based on recorded parameters. These derived parameters are indicated in the plots by a "(D)" symbol in the plot legends and axis titles (e.g., Dynamic Pressure, PSF (D) in Figure 3a). The equations used to calculate the derived parameters are presented in the Appendix.

The sign conventions for the control surface deflections plotted in Figures 2 and 3 are as follows:

Elevator:	Positive trailing edge up.
Stabilizer:	Positive leading edge down.
Rudder:	Positive trailing edge right.
Right Aileron:	Positive trailing edge up.
Left Aileron:	Positive trailing edge up.

The "PT Wheel" plot in Figures 2c and 2f shows the position of the Pitch Trim Wheel in the cockpit. This wheel rotates as the stabilizer position changes.

Chronology of Upset as Determined from DFDR Data

The Flight Data Recorder Group Chairman's Factual Report details the chronology of recorded events preceding the upset. An overview of this chronology is as follows:

The aircraft starts a descent from 24000 ft. with the autopilot in HDG/SEL and V/S modes. During the descent, the Throttle Resolver Angles (TRAs) move from 44° to 37°, and the engine N1s decrease from 85% at the top of descent to about 42% at 19,743 ft., resulting in a descent rate of 2000 ft/min at 235 KIAS.

As the aircraft approaches 16000 ft., the autopilot switches into Capture and then ALT modes, and the plane levels off at 16147 ft., while the TRAs remain at 37°. The aircraft starts to pitch up, the airspeed starts to decrease, and the angle of attack starts to increase. The autopilot moves the stabilizer to keep the airplane in trim as it decelerates.

While level at 16000 ft. and with the TRAs still at 37°, the aircraft starts and completes a right turn with the airspeed still decaying and the angle of attack still increasing. A few seconds later another right turn starts.

As the aircraft rolls through 12° of bank, the TRAs advance to 60° and the airspeed starts to level off at around 178 KIAS. However, the bank angle and angle of attack continue to increase.

As the bank angle passes through 27 degrees, the ailerons start to command roll to the left, but the aircraft continues rolling right. Speed falls from 178 KIAS to a low of 177 KIAS. Angle of attack (α) is 7°. When full left aileron (20°) is reached 3 seconds later, α = 12°.

The stick shaker activates and almost simultaneously the autopilot disconnects (although both events are independent). The TRAs advance to 85°. Left rudder starts to come in at 42° bank, and reaches full deflection about 1.5 s. later. Simultaneously, the bank angle reaches a maximum of 56° and starts to decrease. At this point, CAS = 177 KIAS and α = 13.7 deg.

The aircraft pitches down, and the pitch, yaw and roll Euler angles and flight control surfaces undergo a series of violent oscillations over a period of about 34 seconds.

The oscillations then damp out, the aircraft returns to level flight, and continues on to Miami uneventfully.

III. Simulator Match of the Initial Upset Event

Introduction

To determine whether or not the aircraft motion recorded by the DFDR is consistent with the expected design behavior of the aircraft, the expected behavior in response to the aircraft flight condition and control inputs must first be defined. Defining this predicted motion is a very computationally intensive task, because the number of variables affecting the motion of the aircraft is large, and the values of these variables change with time. Furthermore, the

problem involves solving the six non-linear differential equations of motion of the aircraft simultaneously.

For these reasons, the only practical way to predict the full six degree of freedom motion of the aircraft is with a full flight simulator. The simulator uses mathematical models of the Earth and the aircraft to calculate forces and moments and solve the equations of motion to determine the aircraft position and attitude as a function of time.

This subsection discusses briefly the calculations performed by simulators in general, and the specific methods used by Airbus Industrie to predict the motion of AA903 using the A300 engineering simulator in particular. The approximations inherent in the simulator, and the resulting limitations in the calculated result, are also discussed.

Simulator Modeling - General

The simulator, in essence, solves two non-linear vector differential equations, each of which has three dimensions or components, for a total of six non-linear scalar differential equations. The vector equations are:

$$\bar{F} = \frac{d(m\bar{V})}{dt} \qquad\qquad [1]$$

$$\bar{M} = \frac{d\bar{H}}{dt} \qquad\qquad [2]$$

where $\bar{F}$ is the total force on the aircraft, $\bar{V}$ is the aircraft inertial velocity, $\bar{M}$ is the total moment or torque on the aircraft, $\bar{H}$ is the aircraft angular momentum, m is the aircraft mass and t is time. To solve for the aircraft linear and angular rates and positions, the $\bar{V}$ and $\bar{H}$ terms must be initialized, the $\bar{F}$ and $\bar{M}$ terms must be calculated, and then Equations [1] and [2] must be integrated (once for rates, twice for positions).

The simulator mathematical models are used to calculate $\bar{F}$ and $\bar{M}$ and the aircraft mass properties that define m and the moments of inertia that contribute to $\bar{H}$. These models include:

Atmospheric Model: defines the physical properties (pressure, temperature, density) of the air the aircraft is flying through based on altitude and defined differences from standard day conditions.

Earth Model: defines the acceleration due to gravity and the shape of the Earth (important in navigational problems).

Mass Properties Model: defines the aircraft CG position and moments of inertia about the CG as a function of aircraft gross weight. Sophisticated models can also calculate gross weight based on empty weight and payload and fuel loading scenarios.

Gear Model: defines the forces and moments exerted by the landing gear on the aircraft while the aircraft is on the ground (does not include aerodynamic force increments due to the gear; these are accounted for in the aerodynamics model).

Engine or Thrust Model: defines the total net thrust available from the engines as a function of throttle setting and flight condition.

Flight Controls Model: defines the position of the aircraft flight control surfaces as a function of pilot and/or autopilot control inputs and aircraft flight condition.

Autoflight Model: defines the control inputs commanded by the autopilot as a function of the autopilot programming, mode selection, and aircraft response.

Aerodynamics Model: defines the aerodynamic forces and moments acting on the aircraft as a function of aircraft configuration, flight condition, and control surface deflection.

These models describe the physical quantities they represent only approximately. Some models, such as the Earth model and the Autoflight Model, describe well understood systems and can be very exact. Others, particularly the Aerodynamics model, describe very complicated physical phenomena and therefore involve more simplifying assumptions and approximations and are less exact, or are valid only under certain well-defined conditions.

In general, an aerodynamic model for a simulator is developed by first defining, for steady conditions, the six aerodynamic force and moment coefficients[1] acting on the aircraft as a function of angle of attack, angle of sideslip, aircraft configuration (gear, flap position), Mach number, and control surface deflection. The increments to these coefficients due to aircraft dynamics (angular rates) are then calculated, as well as increments due to aeroelasticity.

In spite of the advance of Computational Fluid Dynamics (CFD), it is not yet feasible to compute in a reasonable time the set of aerodynamic coefficients that depend on every conceivable combination of the independent variables mentioned above. Instead, the steady state force and moment coefficients are measured in wind tunnel tests, while the dynamic terms are calculated based on combinations of CFD and empirical methods rooted in experience. Even so, testing every combination of angle of attack, sideslip angle, flap and gear setting, Mach number and flight control position in the wind tunnel is prohibitively

---

[1] The forces are Lift, Drag, and Side Force. The moments or torques are the Pitching Moment, Rolling Moment, and Yawing Moment.

expensive, and so judgements must be made as to what to test and how to interpolate/extrapolate or otherwise fill in the gaps.

After the development of a predictive aerodynamic model in the wind tunnel, the model is corrected and updated based on flight test results. In this process, the simulator is used to predict the motions measured in flight test, and the models are amended until the simulator correctly reproduces the flight test measurements. Of course, the model can only be updated with confidence in those areas for which flight test results are available, which correspond mostly to the regimes where the aircraft is operated. Less flight data is available at extreme flight conditions, such as stalls, deep sideslips, etc..

In the end, the aerodynamic model generally represents the aircraft extremely well in the flight regimes where the aircraft is normally operated and where a great volume of wind tunnel and flight test data is available for model development. At extreme flight conditions, however, such as large angles of attack and sideslip, there is generally less data available to validate the simulator, and the models in these areas may represent at best an educated guess.

Another important limitation in the simulator aerodynamic model is the assumption of symmetry. On the wind tunnel test stand, the static condition of the aircraft makes the freestream air approach each part of the aircraft at the same angle, and it is valid and convenient to define the aerodynamic coefficients of the entire aircraft in terms of this angle (which will be a combination of angle of attack and sideslip). Because the forces on the entire model are measured, it is not necessary to measure the contribution of each individual aircraft component to these forces and then sum these contributions to get a total effect.[1] Thus the left and right wings, for example, are not modeled separately. In a similar manner, the effect of angular rates is expressed in terms of increments to the aerodynamic coefficients of the whole aircraft, not in terms of increments to airflow angles over separate parts of the aircraft whose independent contributions to the coefficients are then summed. This approach works well when the angular rates are reasonably small and the incremental angles of attack induced on separate parts of the aircraft do not cause flow separation. If, however, the angular rates are large, or if the aircraft is already close to a stalled condition, the incremental angles of attack can cause separation over some parts of the aircraft but not others, resulting in an asymmetrical condition that will not be predicted correctly by the aerodynamic model. Thus, for example, simulators generally do not predict spin characteristics correctly, in which one wing is stalled and the other is still flying.

---

[1] A common exception to this rule is the separate modeling of the horizontal tail; in these "Tail Off" models, the contributions to the aerodynamic forces of the wing-body and the horizontal tail are calculated separately, then summed for the total effect on the airplane. In this discussion, however, we are concerned with the ability of the models to account for asymmetric separated flow on the aircraft, and the conclusions reached in this regard also hold for Tail Off models.

It should be noted that the preceding observations apply most properly to the aerodynamic models of large commercial transports. Simulations of other types of aircraft, such as combat fighters, may employ more sophisticated aerodynamic models that do correctly predict the aerodynamic coefficients acting on the aircraft at extreme flight conditions (which for these planes qualify as "normal" operating conditions).

Because of the limitations inherent in the mathematical modeling of the physics that produces the forces and moments acting on the aircraft, the results of simulator tests must be used with caution when the flight regimes the tests describe approach the boundaries of the areas where sufficient wind tunnel and flight test data is available to validate the simulator. These boundaries are usually defined by large angles of attack (close to stall and higher), deep sideslips (greater than 15°), and high angular rates. Where the simulator models have been validated, they provide an excellent quantitative prediction of the aircraft motion. Where the models have not been validated because of lack of data due to the extreme flight condition, the simulator should be used only as a qualitative predictor of the aircraft motion- e.g., to obtain a general idea of the aircraft response to large control inputs. In very extreme maneuvers, such as those that in a real airplane would result in a spin, the simulator may not be a good indicator of even the qualitative, gross aspects of the aircraft motion.

The DFDR data for the AA903 upset can be described in two parts. In the first part, preceding the first stall, the aircraft motions are smooth and the angles of attack and sideslip are in a range where the aerodynamic model should be valid and it is reasonable to try to duplicate the motion with the simulator. In the second part, after the first stall and during the recovery, the angular rates are very high and the angles of attack and sideslip are frequently outside the range of confidence in the aerodynamic models. In this part of the upset, it is unreasonable to try to reproduce the DFDR recorded motion with the simulator. Instead, the simulator can only be used to obtain qualitative indications of gross aircraft behavior, such as the character of its response to large control inputs. Thus, for example, the simulator can be used to evaluate the merits of various stall recovery techniques even in the regime where the models are inadequate for obtaining a precise, quantitative description of the aircraft motion.

Simulator Matching of Data Recorded in Flight - General

A simulator "matches" a flight test maneuver when it calculates the same aircraft response, or output, to a set of given inputs as recorded on a test aircraft that has received identical inputs. Possible inputs to and outputs from the simulator and test aircraft are as follows:

Inputs:

- Aircraft Configuration: flap and gear positions, weight, CG location, moment of inertia values (or the loading specifications that enable the simulator to calculate these parameters)

- Initial Conditions: altitude, airspeed, linear and angular rates and accelerations at the point where the simulation calculation should start

- Engine Control Parameters: time history data of the throttle position, or N1 value, or thrust value of the engines

- Flight Control Parameters: time history data of the pilot control positions, or the positions of the control surfaces themselves

- Atmosphere: deviations from standard day temperature, time history data of wind magnitude and direction

- External forces or moments (e.g., wake encounters, forces from in flight refueling probes, etc.)

Outputs: Time history data of:

- Aircraft position: altitude and horizontal position
- Aircraft speed: airspeed, rate of climb, velocity components in each axis
- Orientation: Euler angles[1] , angles of attack and sideslip, flight path angle

Note: "Time history data" means the values of a parameter as a function of time.

As can be seen from the above list, the simulator requires a lot of input data in order to correctly compute its outputs. This input data generally comes from the recording system on the test aircraft, which also records the output parameters to which the simulator's computations will be compared. Thus the quality of a simulator match depends not only on the fidelity of the simulator's mathematical models, but also on the accuracy of the flight test data that provides the simulator inputs and targets.

The quality of the recorded flight test data is especially crucial when the simulator matches will be used to update the simulator mathematical models, and numerical accuracy is paramount. Thus flight test aircraft will carry sophisticated sensors and recording equipment capable of sampling data at over 20 samples/ sec., and the recorded data will undergo rigorous scrutiny and correction before being used to generate simulator matches. For accident and incident investigations, the requirement for numerical accuracy is not as great and the sensors and sampling rates of DFDRs are sufficient to describe the

---

[1] The Euler angles are the angles of Pitch, Roll, and Yaw.

aircraft motion and to provide inputs for simulator matches that are meant to confirm the expected behavior of the aircraft, but not serve as bases for updates to simulator math models.

Nonetheless, the limitations of the recorded data must be considered when attempting to analyze the data to obtain information that is not recorded directly but that is inherent in the recorded data. For example, if load factor and airspeed data will be used to estimate winds, the errors associated with each must be taken into account or a very erroneous wind computation may result, even though the recorded load factor and airspeed may give a good indication of the actual values of these parameters. This problem is discussed further in Section D-V and in the Appendix.

The limitations of the recorded data provide another reason to dispense with a simulator match of the second part of the AA903 upset, where the dynamic nature of the motion exaggerates existing problems with the recorded data and introduces new ones, such as data dropouts and pitot-static errors due to large sideslip angles. Problems associated with low sample rates are exacerbated because when the sampled signal changes rapidly, more (unavailable) samples are required to capture those changes. At large sideslip angles and angles of attack, the static ports no longer measure the freestream static pressure accurately and consequently parameters dependent on pressure measurements, such as altitude and airspeed, will be in error. Finally, the dynamic character of the motion can affect the ability of the DFDR to record its information correctly, leading to missing or erroneous data points (for more information on data loss due to dynamic conditions, see the Flight Data Recorder Group Chairman's Factual Report). Because of these errors, the recorded data in the second part of the upset is not as good a quantitative indicator of the aircraft motion as data in the first part, and so comparing questionable simulator data to questionable DFDR data in the second part would be of little value.

Methods used in Simulator Matches of AA903 Pre-Stall Motion

Airbus Industrie attempted to reproduce the aircraft motion measured by the AA903 DFDR during the minute prior to the first stall using the A300 engineering simulator. Three different simulator matches were performed. In the first, no external wind shears or rolling moments were introduced in the simulation; in the second, external wind shears but no external rolling moments were used; and in the third, both external wind shears and rolling moments were used. Each successive match produced better agreement with the motion recorded by the DFDR.

Figures 4a-4c illustrate the methods used to produce each of these matches. The first match (Match A) uses the method outlined above: the simulation is "initialized" at the desired starting point with the proper weight, CG, position, and speed information from the DFDR. Then, time dependent thrust and control surface deflection data determined from the DFDR are used to "drive" the

simulation. The simulation computes the reaction of the aircraft to these thrust and control surface inputs and updates the aircraft position, speed, and attitude parameters accordingly. These parameters are then be compared with the DFDR recorded parameters to determine the quality of the match.

The second match (Match B) uses the same method as the first match, but also uses the differences between the outputs of the first match and the DFDR recordings to generate time-dependent linear winds in order to improve the agreement between the simulator and the DFDR.

The third match (Match C) again uses the same method, but also uses the results of the second match to generate a time-dependent rolling moment coefficient in order to improve the agreement in roll performance between the simulator and the DFDR.

All three Matches begin at a point about 16 seconds before the first stall, just before entering the final right turn before the upset. The reference time used in the simulation (t_{sim}) is related to the Elapsed Time (ET) reference used in this study as follows:

t_{sim}	=	ET	=	MIA ATC Time
0.0 s.		40.0 s.		19:29:00 UTC

The initial conditions for the simulation are set at t_{sim} = 0. as follows:

Weight	=	118,000 kg. = 260,143 lb.
CG	=	29% MAC
Airspeed	=	187 KCAS
Altitude	=	16,100 ft.
Flaps/Gear	=	Up/Up

Simulator Match Results

Figures 5a-5c, 6a-6c, and 7a-7c present the results of simulator Matches A, B, and C, respectively. Time history data for various simulator parameters are plotted and compared to appropriate DFDR data, if available.

Match A shows that in the pitch axis, the simulator starts to deviate slightly from the DFDR recorded pitch angle and angle of attack soon in the maneuver, but agrees with these parameters within 1° until they both reach about 7°. At this point (t_{sim} = 12 s.), the simulator and DFDR bank angles are about 20° and start to deviate significantly from each other; consequently the simulator pitch axis parameters also start to deviate further from the DFDR data. At t_{sim} = 15 s. (slightly before the left rudder input), the simulator has reversed its roll rate and rolled back to 18° of bank, while the DFDR data indicates the roll to the right continued to 40° of bank. Simultaneously, the simulator and DFDR pitch angles have increased to 7.5° and 8.8°, respectively, while the angles of attack have

increased to 7.9° (simulator) and 8.4° (DFDR). As the left rudder is input, the simulator and DFDR pitch axis parameters start to disagree significantly. By 17 s., the DFDR indicates the stall warning has activated, and the DFDR pitch, attack, and bank angles have increased to 14.8°, 13.2°, and 55°, respectively. At the same time, the simulator pitch, attack, and bank angles are 11°, 9.2, and -8°, respectively.

Match B, which incorporates the external winds shown in Figure 8[1] , improves the match of the longitudinal parameters early in the maneuver; pitch angle and angle of attack agree extremely well through t_{sim} = 16 s. This is accomplished primarily by the action of the vertical WZ wind shown in Figure 8, which as it blows from above decreases the angle of attack. This WZ wind ramps in early (starting at t_{sim} = 2 s.) and reaches a maximum value of 5.5 m/s (18 ft/s or 11 kts.) at t_{sim} = 12 s.

The reversal in WZ from t_{sim} = 15 s. to 17 s. occurs as the aircraft is stalling, and Airbus Industrie believes that this effect is an artifice of the uncertainties in the simulation at stall angles of attack and above. In fact, the stall angle of attack in the clean configuration at Mach 0.36 is about 10.9°, and above this angle of attack the simulation may not reflect the actual aerodynamic characteristics of the aircraft. A conservative approach would be to treat simulator data at α = 9° and above as a qualitative indicator of gross aircraft behavior only, and inadequate for deducing the winds or other external influences on the accident flight.

The DFDR data indicates α = 9° at t_{sim} = 15.25 s. = ET 55.25 s. However, the DFDR measures the angle of attack at the alpha vane, which is near the nose and affected by the pitch rate of the aircraft; the α at the CG (which is approximately what the wing sees) reaches 9° almost a second before the α at the sensor (see Figure 3c). Since the aircraft is rolling to the right during the maneuver, the roll rate will induce a higher angle of attack on the right wing than on the left wing. Figure 3c shows that at the right wing tip (y/b = ½), α reaches 9° at about ET = 54 s. = t_{sim} = 14 s., while at that time the α at the CG is only 8° and the α at the vane is 7.5°. Thus separated flow may start to appear over certain parts of the aircraft as early as t_{sim} = 14 s., and this time can be considered the beginning of a transition from confidence in, to a wariness of, the simulator model. For details on the calculation of the αs shown in Figure 3c, please see the Appendix.

While the winds introduced in Match B improve the longitudinal match significantly, they do not resolve the disagreement in roll behavior that starts at

---

[1] These winds could more properly be called "Change in Winds" or "Wind Shears." In addition to the winds shown in Figure 8, there was an approximately steady wind from 250° (True) at about 27 kts. (see Figure 2f). This steady wind affects the aircraft groundspeed and track, but not its motion relative to the air mass, and so for simplicity is not modeled in the simulation. See Section D-V and the Appendix for more information on wind calculations.

about t_{sim} = 12 s. This disagreement indicates that a rolling moment not modeled in Match A or B is acting on the aircraft.

Match C introduces the external rolling moment coefficient (C_l) shown in Figure 9 in addition to the winds shown in Figure 8, and together these elements make the simulator match the longitudinal and lateral DFDR parameters, as shown in Figures 7a-7b. The physical mechanism that generates the external rolling moment is undetermined at this point; the coefficients shown in Figure 9 merely indicate the magnitude of the rolling moment required to force the simulator to match the DFDR data. Some possible sources of an external rolling moment are discussed in Section D-IV.

Just as the winds in Figure 8 are not credible past α = 9° (t_{sim} = 15.25 s.) because of uncertainties in the simulator model, so too the C_ls shown in Figure 9 must be evaluated carefully in this region. While the laws of physics demand that these coefficients act on the aircraft to produce the motion recorded by the DFDR, the source of the coefficients may be different before and after the stall. As the aircraft approaches stall, the rolling motion will make the right wing stall first; the associated loss in lift on that wing will cause a large positive rolling moment, which is probably the source of the very large C_ls shown in Figure 9 after t_{sim} = 15.25 s. Prior to t_{sim} = 15.25 s., the smaller C_ls in Figure 9 are probably due to some other (unknown) cause.

A measure of the magnitude of the C_ls is the lateral control power of the aircraft. At full wheel deflection, the aerodynamic control surfaces will generate a C_l of 0.33; thus the C_l of 0.25 at α = 9° (t_{sim} = 15.25 s.) in Figure 9 is equivalent to about 75% of the lateral control power.

While the C_ls shown in Figure 9 resolve the roll disagreement, Match C is not perfect; there is still a disagreement in the simulator and DFDR heading data[1] starting around t_{sim} = 11 s. (at the point where the roll disagreement in Matches A and B starts). This disagreement suggests that an external, positive (nose right) yawing moment is required in addition to the rolling moment to force a match of the heading traces, and that this yawing moment would appear around the same time as the external rolling moment. Thus both moments may result from the same source. After t_{sim} = 15.25 s., a stall of the right wing before the left wing would produce a large, positive yawing moment.

IV. Aircraft Behavior after the Initial Upset Event

After the first stall, the aircraft underwent a series of violent oscillations in pitch, roll and yaw. As discussed in Section D-III, during this time the angle of attack and, by inference, the sideslip angle frequently exceeded the range in which the simulator aerodynamic models are known to be valid. In addition, the dynamic

---

[1] The simulator and DFDR heading data in Figures 5-7 have been biased so that heading = 0° at t_{sim} = 0. The actual DFDR magnetic heading at t_{sim} = 0. = 19:29:00 MIA ATC time is 237°.

motion causes a number of problems with the DFDR data, including data loss, sampling rate limitations, and erroneous pressure data. For these reasons, there is little value to performing a simulator match of the DFDR data in this region since it would be inappropriate to use the results of such a match to draw any conclusions about the aircraft performance.

Instead, the motion after the first stall can be discussed from a qualitative point of view, to assess whether or not the aircraft reaction was consistent with the control inputs recorded by the DFDR and the gross aircraft handling qualities as determined from flight and wind tunnel tests. In this discussion, the simulator can not provide quantitative information about the aircraft motion, but can provide qualitative information about general trends in the aircraft handling qualities. In what follows, conclusions about the consistency of the recorded motion with the recorded control inputs are based on the experience of Airbus personnel with the aircraft, and on the experiences of the Performance Group members in simulator tests of the upset in the A300 simulator. The results of these tests, and the information they provide about the effect of stall recovery techniques on the post-stall behavior of the aircraft, will be discussed in detail in Section D-VII.

Determination of the First Stall Point

By definition, the aircraft stalls when there is so much separated flow over the wings that an increase in angle of attack does not increase the lift coefficient. In fact, a stall often results in a loss of lift, with a concomitant drop in load factor and a nose-down pitching moment. The A300 flaps up angle of attack for maximum lift at $M=0.36$ is about $10.9°$; Figure 3c shows that the CG sees an angle of attack of $10°$ at ET = 55.5 s., and Figure 3e shows that at this time there is a drop in normal load factor (a "g break.") Simultaneously, Figure 3b shows a drop in pitch rate, evidence of a nose down pitching moment. Thus the first stall can be identified at ET = 55.5 s = 19:29:15.5 UTC. The stall warning activated sometime between 19:29:15 and 19:29:16, or between vane angles of attack of $8.9°$ and $12.1°$[1].

Pitch Response

While the pitch rate drops at ET = 55.5 s., it is still positive for enough time that the pitch angle (θ) and α continue to increase to $16.5°$ and $13.7°$, respectively. At about 19:29:17, both θ and α decrease over a period of 3 to 4 seconds to $-9.1°$ and $2.4°$, respectively, and the stall warning deactivates at 19:29:20.

---

[1] The angle of attack values that bracket the range of time in which the stall warning activated are determined by the word slot locations of the α values and of the stall warning discrete on the DFDR. The stall warning is programmed to activate at $\alpha = 8.5°$; at this point, however, the pitch rate is 4.5°/s (Figures 3b & 3c), and so any delay in the warning or recording system will result in the recorded stall warning discrete triggering at a higher α. Also note that the angle of attack range between the stall warning and actual stall will be reduced if the actual stall angle of attack is reduced, as is the case with spoiler deflection and increasing Mach number.

Starting at 19:29:10, the elevator moves increasingly in the nose-down direction (possibly a reaction by the autopilot to the nose up pitching moment provided by the increasing thrust). After the autopilot disconnect between 19:29:15 and 19:29:16, the elevator continues to move in the nose down direction (which helps break the stall), reaching -8.1° at 19:29:17. The maximum nose down elevator deflection available on the A300 is -15°.

At 19:29:17, the elevator reverses its motion and starts to move in the nose-up direction, reaching 4.9° at 19:29:21. This pitches the aircraft back up into a second stall, which is deeper than the first: α reaches 18.2° at 19:29:23. The elevator again moves nose-down starting at 19:29:21, reaching -7° at 19:29:27, only to reverse again to 8.8° at 19:29:30. Smaller oscillations in elevator position centered around 1° continue until 19:30:00. The pitch response follows and is consistent with these elevator inputs, resulting in three more stall warning activations and angle of attack peaks of 13.8°, 20°, and 15.2°.

As will be discussed further below, the angle of attack excursions are exacerbated by the yawing and rolling oscillations during the recovery. If an aircraft is in a right bank, a nose-left rotation about its vertical axis will raise the nose and increase the angle of attack.

Roll and Yaw Response

The roll and yaw motions of the aircraft are very strongly coupled during the upset. Figure 2e shows that, including the initial rudder input before the first stall, four large, left-to-right rudder inputs were made. While the DFDR does not record sideslip angle (β), it is certain that these rudder inputs resulted in large β's which in turn generated large rolling moments. In fact, the roll oscillations shown in Figure 2e are in phase with the rudder inputs. The aileron traces are also in phase with the roll oscillations, and are coordinated with the rudder, i.e., the aileron and rudder command roll and yaw in the same direction. This coordinated use of almost full roll and yaw control authority resulted in extreme roll rates leading to extreme bank angles, including 83.3° at 19:29:34, and -69.6° at 19:29:38. While the initial continued right roll against left roll control inputs prior to the first stall (discussed in detail in Section D-III) is inconsistent with the expected behavior of the aircraft and justifies the use of the rudder to help stop the roll, the post-stall rolling motion appears consistent with the applied control inputs.

Airspeed Response

At 19:29:08, or about 8 seconds before the first stall, the Throttle Lever Angles (TLAs) advance from 37° to about 65°, so that by the stall the engine N1s have increased from 38% to 105%. At the stall, the throttles are advanced to 84°, and the N1s increase to a maximum of 110%. This increase from idle to full thrust is

reflected in the longitudinal load factor[1] traces (n_x) in Figures 2d and 3e, which show a positive increment in n_x as the N1s increase. Figures 3a and 3e show that the rate of airspeed loss decreases around the same time. Thus the airspeed response is consistent with the increase in thrust.

Note that the n_x trace in Figure 3e is positive and increasing throughout the maneuver, even though the airspeed is decreasing. The seemingly inconsistent n_x trace is the result of both an offset, or bias, in the accelerometer that measures n_x, and of the increasing pitch angle that increases the component of gravity along the aircraft x axis (see the footnote below). In the Appendix, the accelerometer biases along the x, y and z axes are calculated and removed from the accelerometer data. The corrected n_x trace is smaller than the recorded n_x trace, but still positive throughout, which underscores the importance of understanding all the terms that affect load factor data when using that data to draw conclusions about the aircraft performance. The Appendix contains a detailed presentation of the terms that affect the aircraft accelerations and load factors, and describes how to use load factor data to derive aircraft performance parameters not recorded by the DFDR.

After the first stall and during the secondary stalls from 19:29:23 through 19:29:48, the pitch attitude of the aircraft was below the horizon, averaging about -7°, even though the angle of attack was high. This combination of θ and α resulted in a large, negative flight path angle and a loss in altitude. The nose low attitude, together with the high thrust, allowed the airspeed to build to over 250 KIAS at the end of the upset (at about 19:29:58), and allowed recovery to level flight at a low angle of attack (about 2°).

Vertical and Lateral Load Factor Response

The vertical (nlf) and lateral (ny) load factor traces shown in Figure 2d (where they are labeled "Vert. Acc." and "Lat. Acc.," respectively) are consistent with the large oscillations in angular rates throughout the upset. During the first stall, the maximum and minimum nlf excursions are 1.22 and 0.45 g's. During the subsequent oscillations, nlf reached extremes of 2.84 and -0.45 g's, while exceeding 2.0 g's eight times and reaching negative g's four times.

The ny response is consistent and in phase with the rudder inputs, and is characterized by an oscillation about 0 g's with an amplitude of about 0.6 g's and a period of about 8 seconds. The maximum ny excursions recorded are 0.75 and -0.68 g's.

---

[1] The "Longitudinal Acceleration" parameter plotted in Figure 2d is more properly termed the "Longitudinal Load Factor," or n_x. This is the term used in Figure 3e. Similarly, "Vertical Acceleration" and "Lateral Acceleration" are more properly termed "Vertical Load Factor" or "Normal Load Factor" (nlf, or $-n_z$) and "Lateral Load Factor" (n_y). The relationship between the acceleration along an axis i (a_i) and the load factor along the same axis (n_i) is given by $a_i = n_i g + g_i$, where g is the acceleration due to gravity and g_i is the component of gravitational acceleration along axis i.

The longitudinal, vertical, and lateral load factor data shown in Figures 2d and 3e are measured at the accelerometer location, which is near the CG of the aircraft. The rotation of the aircraft about the CG will cause different load factors to be felt at points away from the CG. Figure 10 shows a comparison of the n_x, n_y, and nlf felt at the CG with those felt at the pilot's station and at the rear of the passenger cabin. Data at the pilot station and at the aft cabin could not be calculated from ET = 64 s. to 70 s. because of data dropouts in the DFDR Euler angle parameters, which are needed to calculate load factor increments from the CG (see the DFDR Factual Report for details on these dropouts).

Figure 10 indicates that under dynamic conditions the load factors felt at the ends of the aircraft can be substantially different from those measured at the CG. Figure 10 also indicates that the load factors felt during and immediately after the first stall are moderate compared to those that followed.

The load factors shown in Figure 10 have been corrected for accelerometer bias. For details on this correction and on the calculation of the parameters plotted in Figure 10, please see the Appendix.

V. Discussion of DFDR and Simulator Roll Angle Disagreement

Section D-III described briefly the methods and limitations of using simulations to predict aircraft motion, and presented the results obtained by Airbus Industrie when using the A300 engineering simulator to match the flight parameters recorded by the AA903 DFDR. The simulator matches the DFDR parameters well until shortly before the first stall, at which point the simulator rolls left in response to left roll control input, while the DFDR records the aircraft continuing to roll to the right. The simulator can be made to match the DFDR data by introducing external linear wind shears and an external rolling moment into the simulation. This section discusses possible explanations for the differences in the simulator and DFDR results, and the consistency of these explanations with other information, including that obtained from a careful analysis of DFDR data.

Factors that can cause the simulator to calculate motion that differs from that measured in flight include:

1. Errors in the flight sensors or other measuring/recording equipment.
2. Inaccuracies in the simulator aerodynamic and/or other mathematical models.
3. Improper simulator initialization or matching technique.
4. External forces or moments not modeled in the simulator.

When simulator matches must be performed with the utmost accuracy, as when using the results of the matches to update the simulator aerodynamic models, all four of the factors listed above must be accounted for carefully. In the case of the match of the AA903 event, however, the roll discrepancy is so large that the causes of the discrepancy are not subtle and only the more significant factors in

the list above need to be considered. Thus, only factors (2) and (4) will be discussed at length in this Study. The potential errors introduced by factor (3) are small compared to the roll discrepancy, as are those introduced by factor (1) where comparisons to simulator results are concerned. However, when the DFDR data are used to extract additional information about the flight that is not measured directly, such as wind gust characteristics, then the errors in the recorded data (factor (1)) must be accounted for. The corrections involved are discussed further below and in the Appendix.

Simulator Fidelity

As discussed in Section D-III, much of the roll discrepancy occurs in a region where it is probable that at least one wing is stalled, and where the simulator aerodynamic model is not designed to be representative of the aircraft. Airbus Industrie recommends that the simulator results only be considered accurate up to $\alpha = 9°$, which because of the roll rate may be reached at the right wing tip by ET = 54 s. (see Figure 3c). However, Figure 5c indicates that the roll discrepancy starts at $t_{sim} = 11$ s. (ET = 51 s.), where at the right wingtip $\alpha = 7.2°$ and the simulator models should be accurate. Thus there is at least a three second period where the simulator models are expected to be valid and yet predict a roll behavior substantially different from that recorded by the DFDR. It is this period that is of concern in this discussion.

One possibility that must be considered is that there are inaccuracies in the simulator model even below $\alpha = 9°$. On many aircraft, as α approaches stall the effectiveness of the lateral controls (ailerons and spoilers) starts to deteriorate as separated flow appears near the wing trailing edge and moves forward. However, the A300 simulator models show that the rolling moment coefficient due to full control wheel deflection is actually slightly higher at $\alpha = 10°$ (the stall angle of attack) than it is at $\alpha = 2°$. This somewhat surprising behavior prompted the Performance Group to compare the simulator model with A300 lateral control wind tunnel data. Wind tunnel data was available through $\alpha = 10°$ and indicated that while there is a slight deterioration in roll power at $\alpha = 10°$, the error involved in neglecting this deterioration is small and could not account for the AA903 roll discrepancy[1].

The Performance Group also reviewed simulator matches of flight test roll response maneuvers. The simulator matched all the maneuvers well, even at $\alpha = 7°$, suggesting that the models of the roll control effectiveness in this range is accurate. No matches of roll maneuvers are available above $\alpha = 7°$.

---

[1] The wind tunnel data was taken at Mach = 0.3. The upset occurred at Mach = 0.36. The higher Mach number will decrease the stall angle of attack slightly, and therefore the degradation in the effectiveness of the roll controls will begin at a slightly lower angle of attack than measured in the tunnel. However, these effects are small and do not change the conclusions drawn above.

Airbus provided the Performance Group with data recorded during flight test stalls at conditions similar to those in the accident flight. Both wings-level and turning stall data showed that the aircraft is well behaved in the roll axis throughout the maneuvers, with no sudden roll departures requiring correction with large lateral or directional control inputs. In the turning stall, the bank angle reached 30° and 3° to 5° of rudder was required to coordinate the maneuver just prior to the 'g break.'

The wind tunnel and flight test evidence examined in this investigation indicates that the simulator models the A300 roll control characteristics adequately below α = 9°, and that the flight test aircraft did not exhibit the turning stall roll departure behavior recorded by the AA903 DFDR. The simulator matches presented in Section D-III indicate that a very large decrease in the simulator roll power (up to 75% of normal full lateral control) would be required to generate the rolling moment required to match the DFDR. The wind tunnel and flight test data suggest that it is improbable that the simulator is this much in error.

External Disturbances - General

Another factor that can cause the simulator to compute results different from those recorded by the DFDR data is the action of external forces and moments affecting the aircraft but not modeled in the simulation. Sources of such forces and moments can include:

- Physical differences between the flight aircraft and the modeled aircraft (control rigging differences, aircraft damage, etc.)
- Aircraft contamination (symmetrical/asymmetrical icing, dirt, etc.)
- System failures (e.g., asymmetrical flaps)
- Atmospheric disturbances (wind shears, rotors, updrafts/downdrafts, etc.)
- Contact with another object (e.g., mid air refueling, etc.)

The accident aircraft was inspected after landing and nothing abnormal was found, and so it is unlikely that rigging problems or system failures contributed to an external rolling moment seconds before the aircraft stalled. There is also no evidence to suggest the aircraft hit anything. Therefore the two most likely candidates for an external disturbance include asymmetrical icing and an atmospheric event.

External Disturbances - Asymmetrical Icing

In order for asymmetrical ice formations on the wings to have contributed to the roll behavior, several conditions must have been met:

- The aircraft must have been operating in icing conditions. The evidence collected by other investigative groups for this accident (Operations and Weather) indicates that while the outside air temperature was conducive to icing, it is unclear whether the aircraft was in the clear or in the clouds shortly

before the upset. The DFDR data indicates that the wing anti-ice system was off, although the engine anti-ice system was on. These settings are consistent with flight in conditions conducive to icing, but no ice accumulations observed by the crew. The settings are also consistent with American Airlines operating procedures, which require use of engine anti-ice when conditions conducive to icing exist in order to prevent entering actual ice-accreting conditions with engine anti-ice turned off.

- There must have been some mechanism by which the ice formations on the left and right wings differed substantially. In order for ice to produce a roll to the right, the ice on the right wing must be more effective at spoiling lift and control surface effectiveness than the ice on the left wing.

- The effect of the ice must be significant only at $\alpha = 7°$ and above. Since the simulator duplicates the roll behavior well to $\alpha = 7°$, the ice must have no effect on the rolling moment below this α. Furthermore, the DFDR data indicates that no aileron deflection (roll control input) is required to trim wings level flight before or after the upset, indicating symmetrical lift from both wings.

It is difficult to evaluate the probabilities of each of these criteria because both the formation of ice shapes and their effects on the aircraft are difficult to predict with accuracy[1]. However, in general an aircraft flying through a homogeneous icing environment at close to 0° sideslip will accumulate ice symmetrically on both wings. This ice lowers the stall angle of attack, while leaving the lift curve slope relatively unaffected. Thus the effect of ice on lift is not perceived until the α exceeds the new, lower stall α (the effect of ice on drag, however, is significant at all angles of attack).

One possible mechanism for obtaining asymmetrical ice formations is by having the ice accumulate symmetrically, but then shed asymmetrically. While the physics of ice shedding are far too complicated for any kind of significant analysis, it is not unimaginable that the distribution of light and shadow and other variables that affect temperature could cause temperature gradients over the aircraft that result in ice being shed more quickly from one wing than the other. Because the ice affects only the maximum lift obtained from the wing and not the lift curve slope, the asymmetry has no effect until high α.

External Disturbances - Wind Shears/ Vortices/ Turbulence

This subsection discusses how disturbances in the atmosphere (changes in wind direction and velocity) can affect the aircraft motion, and describes briefly the

---

[1] Ice shapes on unprotected areas (those without anti-ice treatment) of the A300 ancestor aircraft wing and tail were flight tested during certification. These tests showed no significant effects of ice on the lift characteristics.

physical characteristics and sources of some of these disturbances. The effects, characteristics, and sources of vortices are given special attention because of the ability of a vortex to roll an aircraft. An attempt to identify traces of an atmospheric disturbance through analysis of the DFDR data is also discussed, as is the consistency of an atmospheric disturbance with the weather encountered before and after the upset, and reported by other aircraft.

"Wind" is the movement of air relative to the Earth. In a constant wind, all parts of the air mass have equal speed and direction, and the performance of the aircraft *relative to the air* is the same as if the wind were calm. A variable wind will change velocity and/or direction as a function of time and/or space. A *gust* is a change in wind as a function of time, and a *wind shear* is a change in wind as a function of space or position. If these gusts and shears are sudden enough, they can induce significant changes in the angles of attack and sideslip of the aircraft or of different aircraft components, and disturb the aircraft attitude. *Turbulence* describes gusts and shears that are random in nature, so that the average change in wind due to the gusts and shears over a long time or large distance is small, even though wind changes over a short time or small distance can be large.

For a wind to generate the sustained rolling moment coefficient (C_l) shown in Figure 9 (up to α = 9°), the gusts and shears must provide an angle of attack difference between the left and right wings that steadily increases over 4 seconds. The angle of attack of the left wing must be greater than that on the right wing, requiring an updraft on the left wing or a downdraft on the right wing or both. This amounts to a difference in the vertical component of the winds between the left and right wings, or a vertical shear in the wind over the wingspan of the aircraft.

The sustained nature of the required wind shear makes it unlikely that is the result of turbulence, particularly in light of the "intermittent light chop" character of the turbulence up to the upset (Figure 3e shows nlf excursions of ±0.03 g's and Figure 3c shows α excursions of about ±0.2°). The required wind shear is more characteristic of an organized flow structure in the atmosphere, such as a vortex. Air in a vortex moves in a circular pattern around a central core, so that the air at diametrically opposed points of the circle moves in opposite directions. Examples of vortices include tornadoes, water flowing down a drain, and the flow structures shed from the wingtips of airplanes.

Figure 11 illustrates how a vortex can induce different angles of attack on the left and right wings, thereby causing a rolling moment. A measure of the magnitude or strength of a vortex is the induced wind shear velocity at a representative location. Airbus estimates that a vortex that generates a 5 m/s (16 ft/s) shear at the wing mean aerodynamic chord (about 10 m (33 ft) from the centerline) is sufficient to produce the C_l shown in Figure 9.

Horizontal vortices as illustrated in Figure 11 can be generated in the wakes of airplanes, by strong winds flowing over mountainous terrain (mountain rotors), and in the vicinity of convective activity such as thunderstorms. An encounter with a vortex can seriously disrupt the attitude of an aircraft. Note, however, that the scale of the vortex must be such that it can induce opposite velocities over a distance on the order of the wingspan of the aircraft; if a vortex is large compared to the aircraft, the velocities induced on the left and right wings will not differ greatly and no rolling moment will result.

At the time of the upset, AA903 was at 16,000 ft off the Florida coast, where an encounter with a mountain rotor is unlikely. Furthermore, a survey of the flight paths of other aircraft in the area at the time indicates that it is also unlikely that AA903 encountered a wake vortex. Figure 12 shows Miami ARTCC radar tracks of AA903 and surrounding flights around the time of the event. This Figure shows that 19:29:15 UTC Miami ATC time, the only aircraft near AA903 is the one with Beacon Code 677, and that aircraft is *behind* AA903, making it impossible for AA903 to have passed through its wake.

The Weather Group Chairman's factual report indicates that there was strong convective activity upstream of the general area where AA903 experienced the upset. While neither AA903 (before the upset) nor any other flight in the area reported any turbulence greater than "light chop," it is possible that the convective activity in the area could have produced wind shears of the magnitude required to produce the rolling moment shown in Figure 9. However, the required 5 m/s wind shear from the centerline of the airplane to the mean aerodynamic chord (or 10 m/s shear from the left MAC to the right MAC), while theoretically possible, would be considered unusual for the weather of that day. This amount of shear is sufficient to affect the roll performance of the airplane significantly only if the angle of attack is very close to stall; as discussed in Section D-VI, the same amount of wind shear has a minimal effect on roll performance if encountered at a higher airspeed and lower angle of attack.

In addition to an external rolling moment (from whatever source), to match the DFDR data the simulator requires the longitudinal, lateral, and vertical wind shears at the aircraft CG shown in Figure 8. However, these shears do not play a significant part in the roll departure, and so in this sense are less significant than the rolling moment. Nonetheless, if the external rolling moment is due to an atmospheric disturbance, the simulator indicates that the disturbance must not only produce shears at the left and right wings that generate the rolling moment of Figure 9, but simultaneously produce the shears at the CG shown in Figure 8. Even if the shears shown in Figure 8 are not exactly those induced on the aircraft, it is certain that a vortex encounter will induce *some* wind shear that will be felt at the CG. In the condition illustrated in Figure 11, where the aircraft centerline coincides with the vortex core, there are no winds induced at the CG. However, the aircraft has to enter and leave the vortex, and at these times shears along the aircraft centerline will appear as the centerline passes through

the rotating part of the vortex. It is also likely that the passage into and out of the vortex will be associated with increased turbulence.

Consistency of an Atmospheric Event with DFDR Data

The DFDR data can be used to estimate the wind shears felt along the centerline of the airplane, assuming that all points along the centerline feel the same wind. These estimated shears can then be compared with the shears of Figure 8 and/or other shears that would be associated with an atmospheric disturbance. Such an analysis of the AA903 DFDR provides no conclusive evidence of a disturbance in the wind other than a shift in wind direction, and therefore does not support the scenario of a vortex encounter or other atmospheric event.

The wind is the difference between the aircraft motion relative to the Earth and its motion relative to the air, as reflected in the following vector equation:

$$\bar{V}_G = \bar{V}_A + \bar{V}_{A/G} \qquad\qquad [3]$$

where $\bar{V}_G$ is the aircraft velocity relative to the ground, $\bar{V}_A$ is the aircraft velocity relative to the air, and $\bar{V}_{A/G}$ is the air velocity relative to the ground (the wind).

The motion of the aircraft relative to the Earth is measured by the inertial accelerometers, and the motion of the aircraft relative to the air is measured in part by the airspeed system and the angle of attack vane. To completely define the motion relative to the air, the sideslip angle (β) must be known. While the aircraft is not equipped to measure and record β, β can be estimated using the lateral load factor and the estimated side force characteristics of the airplane.

The Appendix presents the details of the calculations of the terms needed to solve Equation [3] for the wind speed. The results are shown in Figure 13, which compares the calculated winds with the winds computed by the Flight Management Computer (FMC) and recorded by the DFDR. The calculated winds are probably more accurate because they are based on load factor data, which has a higher sample rate than the FMC wind data. Also, the calculated winds account for the effect of sideslip angle, whereas the FMC winds do not. In any case, the FMC and calculated winds agree well, and show a wind shift to the North at ET = 48 s. The sudden changes in wind direction after ET = 54 s. are not realistic and simply reflect the strong lateral acceleration response to the rudder input.

Figure 13 also compares the wind shears shown in Figure 8 with the calculated and DFDR recorded winds. The Figure 8 winds have been transformed into Direction and Velocity components, and summed with a constant baseline wind from 248° at 30 kts. (remember, the Figure 8 winds are really wind *shears* or changes in wind, and so these changes must be added to the baseline wind to get the actual total wind). While the calculated winds show a wind shift to the

North, the simulator winds show a shift to the South. A wind shift to the South will move the sideslip angle in the negative direction; this may account for the simulator heading lagging behind the DFDR heading in Figures 6c and 7b.

At around the time of the wind shift, Figure 13 shows about a 6 ft/s decrease in the vertical wind. This decrease is substantially less than the vertical wind shear used in the simulator matches. It is interesting to note that the calculated vertical wind shows a relatively constant 4 ft/s downdraft soon after the level off at 16,000 ft., at around ET = 15s. This apparent downdraft can also be the result of small errors in the α vane measurement or calibration; for example, if the actual α were 0.5° higher than the recorded α, the wind calculation would predict zero vertical wind at that time.

The shift in vertical wind at ET = 48 s. coincides with an increase in the pitch rate (see Figure 3b). Thus it is possible that the angle of attack data in this region is contaminated by pitch rate effects, either because the induced angle of attack at the vane is not entirely corrected for (see the Appendix), or perhaps because the inertial properties of the α vane are affecting its motion. Even if the downdraft is real, it is small compared to the 16 ft/s wind shear that a vortex must generate at the wing MAC in order to roll the aircraft.

The results of Figure 13 show a shift in the wind direction shortly before the upset, but do not show a significant change in the vertical wind or in the wind speed. While it is difficult to predict effects an encounter with a vortex would have on the aircraft airspeed system, angle of attack vane, and CG trajectory, it is not unreasonable to expect that a disturbance in these items would result from such an encounter. This disturbance would in turn be reflected by a disturbance in the calculated winds. The shift in wind direction is evidence for unsteadiness in the airmass, but can not be said to be conclusive evidence of a vortex or wind shear. The strongest evidence of a vortex encounter should appear in the angle of attack and consequently the vertical wind, as the nose of the aircraft passes through the rotational part of the vortex. A vortex of the magnitude required to roll the aircraft will generate 16 ft/s shears at about 30 ft. from the vortex center; thus as the α vane passes though these shears, the vertical wind calculation should result in a 16 ft/s updraft or downdraft. The strongest actual downdraft calculated from the DFDR data is only 6 ft/s, and as mentioned above, even this value may reflect pitch rate effects on the α vane. Thus the wind calculations based on the parameters recorded by the DFDR do not provide any evidence for an airmass disruption other than a shift in the horizontal wind.

The absence of an atmospheric disruption is consistent with the turbulence level before and after the upset, and with the experience of other flights in the area. According to the Operations Group Factual Report, the crews of these flights did not report any turbulence greater than an "intermittent light chop."

VI. Significance of the Roll Angle Disturbance in the Upset Event

The previous section discussed possible explanations for the disagreement between the simulator and DFDR roll angle behavior. While there is insufficient consistent information to determine conclusively the reasons for the roll departure, such knowledge is not required to discuss the significance of the roll departure in the mechanics of the overall upset. This section describes the general effect of a roll disturbance on the performance of the aircraft, and presents the results of pilot-in-the-loop simulator evaluations of the effect of a roll disturbance on the aircraft handling qualities at various flight conditions.

When the autopilot switches into ALT mode after capturing 16,000 ft., it starts using elevator and stabilizer control inputs to try to maintain that altitude. Since the throttles remain at or near idle during this time, drag exceeds thrust and the aircraft starts to decelerate. Consequently, the autopilot starts to pitch the aircraft up in order to increase the angle of attack and maintain the lift required for level flight at 16,000 ft. At the bottom of the descent (about 19:28:25), the airspeed is 215 KIAS and α is 3°. At 19:29:12, the airspeed has decreased to 178 KIAS and α has increased to 7°. The roll angle at this point is 23° and starts to increase as the roll disturbance takes effect. The average rate of change of α ($d\alpha/dt$) up to this point is 0.085°/s.

As the aircraft rolls, the vertical component of the lift vector that supports the aircraft weight starts to decrease, and so the total lift must increase in order to maintain level flight. Figure 3c shows that shortly after the onset of the roll disturbance at approximately 19:29:12, $d\alpha/dt$ increases sharply to about 1.5°/s and then to about 4°/s shortly before the stall. This brings α from 7° to 10° (the stall α) in about 3.5 s. Had $d\alpha/dt$ remained at 0.085°/s, it would have taken another half a minute to exceed the stall α. This would perhaps been enough time for the thrust application at 19:29:08 to have reversed the deceleration and avoided the stall.

The significance of the roll upset in the mechanism of the first stall is that the rapid increase in bank angle required a rapid increase in α (a large $d\alpha/dt$) in order to maintain level flight. Because the airspeed at the time of the roll upset was low, and consequently the α was already high, the large $d\alpha/dt$ increased the α beyond stall in very little time.

Effect of Initial Flight Condition

It is of interest to determine the effect of initial airspeed on the roll and stall scenario just described. Intuitively, a higher airspeed will have the following benefits:

- The initial angle of attack will be lower, leaving a greater margin to stall.
- The effectiveness of the control surfaces will be increased because of the higher dynamic pressure.

- If the external rolling moment is caused by a vortex, the induced angles of attack and hence the rolling moment will be reduced.

A more subtle benefit of a higher airspeed is the increased lift increment per change in α (dL/dα). This effect enables the aircraft to obtain the increased lift required in a bank with less of a change in α than is required at a lower airspeed, thereby preserving a greater margin to the stall α. The effect can be seen from the following relationships:

The lift of the airplane is given by

$$L = \frac{1}{2}\rho V^2 C_L S = \frac{1}{2}\rho V^2 a(\alpha - \alpha_0)S \qquad [4]$$

where

L = Total Lift
ρ = Air Density
V = True Airspeed
C_L = Lift Coefficient
S = Wing Reference Area
a = Lift Curve Slope (dC_L/dα)
α_0 = Angle of Attack for Zero Lift

It follows from Equation [4] that the change in total lift with α is

$$\frac{dL}{d\alpha} = \frac{1}{2}\rho V^2 aS \qquad [5]$$

Note the dependence of dL/dα on the *square* of the airspeed; thus increasing the airspeed by 10% increases dL/dα by 21%. If the α required for level, 1g flight is α_{1g}, Equation [4] indicates that

$$\frac{1}{2}\rho V^2 aS = \frac{W}{\alpha_{1g} - \alpha_0} \qquad [6]$$

where W is the aircraft weight. Substituting [6] into [5] gives

$$\frac{dL}{d\alpha} = \frac{W}{\alpha_{1g} - \alpha_0} \qquad [7]$$

which again shows that dL/dα increases with higher airspeeds and lower α_{1g}.

To further evaluate the effect of the initial flight condition on the consequences of the bank angle disturbance, the wind shears shown in Figure 8 and the external

rolling moment shown in Figure 9 were modeled in the A300 engineering simulator. These items were then activated at appropriate times during the simulations, thereby providing a bank angle upset from which the pilot (or autopilot) would have to recover. These simulations provided a means for determining the effect of both initial airspeed and stall recovery techniques on the motion of the aircraft. The effects of stall recovery techniques are discussed in Section D-VII.

The effect of initial airspeed was tested by comparing the results of the following simulator scenarios:

Scenario 1. The aircraft is initialized on the descent with the autopilot set up to capture and hold 16,000 ft., and with the autothrottles engaged and set up to hold 210 kts. A short time after leveling off at 16,000 ft., a 30° heading change is issued to the autopilot. As the bank angle passes through 20°, the external rolling moment (ΔC_l) is activated and the autopilot is left free to control the resulting upset.

Scenario 2. The aircraft is initialized as in Scenario 1., but with the autothrottles disengaged and the thrust levers at idle. After the aircraft levels off, it is allowed to decelerate at idle thrust. The 30° heading change is issued to the autopilot at a time that will result in a 20° bank angle as the aircraft decelerates to 178 kts. When the airspeed reaches 180 kts., the throttles are advanced manually to full thrust. At 178 kts., the ΔC_l is activated and the recovery left to the autopilot.

In both these Scenarios, it is assumed that if the α exceeds 10° then the autopilot is unable to control the bank upset and a stall results. Because of the limitations of the simulation described in Section D-III, simulator data taken after α exceeds 9° is considered unreliable for determining the ability of the autopilot to control the aircraft. Also because of this limitation, the ΔC_l modeled in these simulations represents only that portion of the external rolling moment shown in Figure 9 that corresponds to $\alpha < 9°$. After reaching a peak value of 0.25, the ΔC_l ramps to zero over 2 seconds.

Strictly speaking, the external winds shown in Figure 8 are questionable after t_{sim} = 15 s., since they are based on simulator matches at times where $\alpha > 9°$. Nonetheless, in these simulations the entire wind profile as shown in Figure 9 is used. This leads to misleading α data at the point (t_{sim} = 15 s.) where WZ drops suddenly from 5.5 m/s to -5 m/s over 3 seconds; a more realistic estimate of α at these times is to use the difference between the pitch angle and the flight path angle. This is the α used in the discussions that follow.

The results of Scenario 1 indicate that when the ΔC_l is encountered at 210 kts. and a 20° bank angle, the bank angle is disturbed further to about 42° before the autopilot arrests the roll while using about 35° of control wheel deflection. The maximum α achieved during the encounter is about 7° (well below stall).

The results of Scenario 2 indicate that when the ΔC_l is encountered at 178 kts. and a 20° bank angle, the bank angle is disturbed further to about 40°, at which point α exceeds 10° and the assumption is that the aircraft stalls. This behavior is similar to that recorded by the DFDR. In the simulation, the autopilot is able to arrest the roll at 45°, though α reaches a maximum of about 12°; in reality, the wings probably stall asymmetrically, resulting in a further bank angle disturbance as reflected in the DFDR data.

VII. Effect of Stall Recovery Technique on Aircraft Motion

The simulations described in Section D-VI were also used to evaluate the effect of manual stall recovery technique on the aircraft motion. For these cases, the simulation is set up as in Scenario 2 of Section D-VI, and at the time the ΔC_l is activated the flying pilot is invited to disconnect the autopilot and recover the aircraft manually. The effects of different recovery techniques- i.e., the selection, sequence, and magnitude of control inputs- can then be observed.

The recovery techniques studied in this way fall into two categories:

A. Attempts to duplicate the objectives and control input characteristics of the recovery technique recorded by the AA903 DFDR. The Operations Group Factual Report indicates that at the time of the upset, the crew initiated a "microburst escape" maneuver, which involves maintaining maximum thrust and a target pitch attitude of 20° until the aircraft is out of danger. This is reflected in the DFDR elevator traces which show nose up control inputs after the nose dropped following the first stall. Independently of the escape maneuver, roll control in these cases is attempted by using large rudder inputs in concert with large wheel inputs, as reflected in the DFDR data.

B. Attempts at recovery by first lowering the angle of attack and then leveling the wings, using various combinations and magnitudes of lateral and directional control inputs.

As noted in Sections D-III and D-IV, the fidelity of the simulator aerodynamic model in the flight regimes of interest in the present discussion is questionable; the model is not designed to account for the effects separated flow and extreme angular rates and airflow angles. Therefore, the simulator can not be used to predict a *quantitative* or precise description of the aircraft motion in these regimes; it can, however, be used to obtain a *qualitative* or "order of magnitude" indication of the gross aircraft handling qualities and responses to various control inputs. In this way the simulator is a useful tool in determining the merits and shortcomings of the general recovery techniques described above.

The response of the simulator to the Category A recovery techniques is similar to that recorded by the DFDR. Repeated nose up pitch commands in an attempt to capture and maintain a pitch attitude of 20° result in secondary stalls and delay

the eventual recovery to level flight. Simultaneously, the use of almost full wheel and rudder inputs result in overcorrection and poor roll control, with the bank angle and roll rate oscillating between large positive and negative values (±40° and ±30°/s). In addition, large rudder inputs while the aircraft is banked raise the nose to large pitch angles that result in large angles of attack when the aircraft rolls through wings level, thereby exacerbating the stall problem.

The response of the simulator to the Category B recovery techniques indicates that the recovery of bank angle and airspeed is accomplished most effectively by pitching and keeping the nose down to lower the angle of attack below stall while using coordinated lateral and directional controls to level the wings. The altitude loss involved in lowering the nose until sufficient airspeed is recovered is much less than the 3000 ft. lost during the secondary stalls and lateral-directional oscillations experienced by AA903.

The Category B results also indicate that careful use of the rudder to recover the bank angle when the lateral controls are ineffective is appropriate (e.g., while the wings are stalled or under the influence of the external rolling moment). Rudder pedal deflections of 5° are sufficient for this purpose; full 15° pedal deflections result in the roll control problems associated with the Category A results.

E.   CONCLUSIONS

The evidence presented and analyzed in this Performance Study indicates that after descending to 16,000 ft., AA903 slowly decelerated until the angle of attack exceeded the angle of attack for maximum lift and the aircraft stalled. Following the nose down pitching motion associated with the stall, the aircraft pitched nose up in response to elevator commands, increasing the angle of attack into a secondary stall. This cycle was repeated three more times for a total of five excursions above the stall angle of attack.

During these pitch oscillations, the aircraft underwent large oscillations in the lateral and directional axes in response to full coordinated lateral/directional control inputs. The oscillations about all three aircraft axes resulted in large longitudinal, lateral, and vertical load factors at the aircraft CG. Control of the aircraft was regained when the airspeed increased to the point that the pitch excursions no longer increased the angle of attack beyond stall.

Prior to the first stall, the aircraft was in a right turn. In spite of left roll control commands by the autopilot, the bank angle departed to the right and reached 56° before it was arrested with left rudder inputs just as the aircraft reached stall. The effect of the bank angle disturbance is to increase the lift required for level flight and accelerate the rate at which the angle of attack increases, thereby shortening the time required to exceed the stall angle of attack.

The roll behavior recorded by the DFDR prior to the stall does not reflect the expected handling characteristics of the A300, as represented by the A300

engineering simulator. The simulator responds to the same lateral control inputs as recorded on the accident flight by rolling promptly back to wings level.

While a significant part of the simulator/DFDR roll disagreement corresponds to high angle of attack conditions where separated flow is likely on at least one wing and where the simulator is not expected to represent the airplane, the initial part the roll disagreement occurs around $\alpha = 7°$, where the evidence suggests that the simulator is an adequate representation of the aircraft. DFDR disagreement with an accurate simulation is consistent with external effects acting on the aircraft that are not modeled in the simulator, such as wind shears produced by an atmospheric disturbance. Airbus Industrie was able to duplicate approximately the motions recorded by the DFDR in the simulator by introducing such wind shears, together with an external rolling moment, into the simulation.

An atmospheric disturbance should also affect other aircraft parameters, such as α, load factors, and airspeed, and therefore be detectable through an analysis of the DFDR data. However, the analysis of the DFDR data described in this Study reveals that while the airplane was flying in about a 30 kt. Southwest wind, there is little evidence of a disturbance in that wind field, other than a shift in the wind direction, near the time of the upset.

The lack of DFDR evidence for a disturbance in the wind field, together with the inconsistency of such a disturbance with the turbulence levels of the accident flight before and after the upset and with the turbulence experienced by other aircraft in the area, make it difficult to conclude positively that AA903 encountered an atmospheric disturbance prior to the upset, although this remains a possibility.
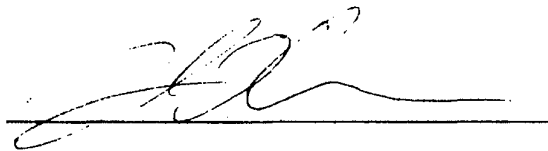
Another possible explanation for the simulator and DFDR disagreement is asymmetric ice contamination on the wings. However, there is insufficient information available to evaluate the likelihood of this possibility.

It is unlikely that continued analysis of the information available for AA903 will yield any further insights into the cause of the roll departure. At this point, the most expeditious way to determine whether an external influence (such as ice contamination or an atmospheric disturbance) is necessary to produce the roll departure is to flight test the roll behavior of the accident aircraft near stall angles of attack. Such a test would also indicate if characteristics of the individual airplane, such as control rigging, can contribute to anomalous roll behavior near stall.

Nevertheless, such a flight test is not necessary. Conclusive knowledge of the reasons for the roll departure is not required to evaluate the significance of the departure in the mechanics of the overall upset, or to determine its effects on the aircraft motion if encountered at a different initial condition. On the accident flight, the roll departure resulted in a stall because the aircraft was flying at an airspeed that did not allow sufficient angle of attack margin to increase the lift as

necessary to compensate for the increased bank angle. Simulator tests indicate that had the roll upset been encountered at an airspeed of 210 kts., the event could have been controlled easily by the autopilot.

Simulator tests also indicate that the control techniques used to recover from the stall have a strong effect on the post stall motion. Techniques that attempt to maintain a nose-high attitude while controlling bank angle with large rudder and wheel inputs result in the secondary stalls and large lateral/directional oscillations experienced by AA903. Techniques that attempt to first lower the nose and angle of attack and use small, coordinated rudder and wheel inputs result in a quicker and smoother return to controlled, level flight.

John J. O'Callaghan
Aerospace Engineer - Vehicle Performance
National Transportation Safety Board

June 30, 1998